ADVANCES IN ATMOSPHERIC SCIENCES, VOL. 31, NOVEMBER 2014, 1331–1342

Impacts of Uncertainty in AVOC Emissions on the Summer RO_x Budget and Ozone Production Rate in the Three Most Rapidly-Developing Economic Growth Regions of China

WANG Feng[1,2,3], AN Junling*[1], LI Ying[1], TANG Yujia[1,2], LIN Jian[1,2], QU Yu[1], CHEN Yong[1], ZHANG Bing[3], and ZHAI Jing[3]

[1]*State Key Laboratory of Atmospheric Boundary Layer Physics and Atmospheric Chemistry, Institute of Atmospheric Physics, Chinese Academy of Sciences, Beijing* 100029

[2]*University of Chinese Academy of Sciences, Beijing* 100049

[3]*Anhui Meteorological Bureau, Hefei* 230061

(Received 19 December 2013; revised 16 April 2014; accepted 05 June 2014)

ABSTRACT

High levels of uncertainty in non-methane volatile organic compound (NMVOC) emissions in China could lead to significant variation in the budget of the sum of hydroxyl (OH) and peroxy (HO_2, RO_2) radicals (RO_x = OH + HO_2 + RO_2) and the ozone production rate [$P(O_3)$], but few studies have investigated this possibility, particularly with three-dimensional air quality models. We added diagnostic variables into the WRF-Chem model to assess the impact of the uncertainty in anthropogenic NMVOC (AVOC) emissions on the RO_x budget and $P(O_3)$ in the Beijing–Tianjin–Hebei region, Yangtze River Delta, and Pearl River Delta of China. The WRF-Chem simulations were compared with satellite and ground observations, and previous observation-based model studies. Results indicated that 68% increases (decreases) in AVOC emissions produced 4%–280% increases (2%–80% decreases) in the concentrations of OH, HO_2, and RO_2 in the three regions, and resulted in 35%–48% enhancements (26%–39% reductions) in the primary RO_x production and $\sim$ 65% decreases (68%–73% increases) of the $P(O_3)$ in Beijing, Shanghai, and Guangzhou. For the three cities, the two largest contributors to the RO_x production rate were the reaction of O^1D + H_2O and photolysis of HCHO, ALD2, and others; the reaction of OH + NO_2 (71%–85%) was the major RO_x sink; and the major contributor to $P(O_3)$ was the reaction of HO_2 + NO ($\sim$ 65%). Our results showed that AVOC emissions in 2006 from Zhang et al. (2009) have been underestimated by $\sim$ 68% in suburban areas and by $>$ 68% in urban areas, implying that daily and hourly concentrations of secondary organic aerosols and inorganic aerosols could be substantially underestimated, and cloud condensation nuclei could be underestimated, whereas local and regional radiation was overestimated.

Key words: volatile organic compounds, RO_x, ozone, WRF-Chem model

Citation: Wang, F., and Coauthors, 2014: Impacts of uncertainty in AVOC emissions on the summer RO_x budget and ozone production rate in the three most rapidly-developing economic growth regions of China. *Adv. Atmos. Sci.*, **31**(6), 1331–1342, doi: 10.1007/s00376-014-3251-z.

1. Introduction

In recent decades, megacities and city clusters in China, especially the Beijing–Tianjin–Hebei region (BTH), Yangtze River Delta (YRD), and Pearl River Delta (PRD) have experienced rapid economic growth. The rapid economic development and urbanization has led to a serious deterioration in air quality (Shao et al., 2006; Zhang et al., 2008; Gao et al., 2011). Among the air pollution issues, photochemical smog is one of the major types responsible for air quality degradation (Chameides et al., 1992; Sillman, 1999). Volatile organic compounds (VOCs) play a significant role in the formation of ozone (O_3) and secondary organic aerosols (Carter, 1994; Avery, 2006). Field campaigns and modeling studies have extensively recorded many aspects relating to these issues. For example: the complex nonlinear relation between O_3, nitrogen oxides (NO_x) and VOCs (Sillman, 1999; Kleinman, 2005); the impact of VOC emissions on the quantities of hydroxyl (OH) and peroxy (HO_2, RO_2) radicals (RO_x = OH + HO_2 + RO_2) (Thornton et al., 2002; Ma et al., 2012), which are central players in atmospheric chemistry and initiate and participate in almost all of the complex chemical pathways in the atmosphere (Mao et al., 2009; Lu et al., 2012); the ozone production rate, $P(O_3)$ (Kleinman, 2005; Chen and Brune, 2012); the ozone production efficiency (Kleinman et

* Corresponding author: AN Junling
Email: anjl@mail.iap.ac.cn

al., 2002; An, 2006; Chou et al., 2009; Xu et al., 2009); and O_3 sensitivity assessments using the radicals budget (Kleinman, 2005).

Air quality modeling is a key tool for assessing the impact of emission control strategies on ambient pollutant levels, as well as determining whether a geographic area is attaining an air quality standard in response to emissions reductions; and issues related to this have been extensively documented in China (Hao et al., 2000; Fu et al., 2009; Tie et al., 2009; Liu et al., 2010; Wang et al., 2010; Xing et al., 2011). However, considerable uncertainties still exist in terms of anthropogenic VOC emissions over China. Streets et al. (2003) estimated the overall uncertainty in non-methane VOC (NMVOC) emissions in Asia for the year 2000 to be ±130%. Zhang et al. (2009) updated this emission inventory with some improved methods, and the uncertainty in NMVOC emissions in China for the year 2006 was subsequently reduced to ±68%. Wei et al. (2008) compiled an emissions inventory of NMVOC in China for the year 2005 and estimated an uncertainty of −44% to 109%. Bo et al. (2008) established another NMVOC emissions inventory in China for the year 2005 with an uncertainty of −36% to 94%. Zheng et al. (2009) and Huang et al. (2011) developed an emissions inventory of NMVOC in the PRD for the years 2006 and 2007, and estimated the uncertainties to be in the ranges of −50% to 120% and −133% to 133%, respectively. Substantial uncertainties in the NMVOC emissions in China could produce significant variation in the RO_x budget and $P(O_3)$. However, to the best of our knowledge, few studies in China have focused on these issues. Accordingly, in the present reported study, our aim was to evaluate the effects of the uncertainty in the anthropogenic NMVOC (AVOC) emissions inventory developed by Zhang et al. (2009) on the RO_x budget and $P(O_3)$ in the BTH, YRD, and PRD, and present some implications for underestimation of AVOC emissions. Furthermore, the WRF-Chem simulations were compared with satellite observations, ground measurements of OH and HO_2, and previous studies with observation-based models.

2. Data and methods

2.1. *Observational data*

In this study, the observed air temperature (TA) and relative humidity (RH) at 2 m above the ground, and wind speed (WS) and direction (WD) at 10 m above the ground were from the National Climatic Data Center, China Meteorological Administration (Zhang et al., 2012). There were ∼ 700 stations with hourly observations in domain 1 (Fig. 1). Observed concentrations of O_3 and NO_x at six stations over the BTH were obtained from the Beijing Atmospheric Environmental Monitoring Action carried out by the Chinese Academy of Sciences (CAS) (Li et al., 2011). Measurements of OH and HO_2 at the Guangzhou Backgarden station (23.487°N, 113.034°E) of the PRD were taken from Lu et al. (2012). Formaldehyde (HCHO) is an important indicator of tropospheric VOC emissions, since it is a principal intermediate in the oxidation of VOCs in the troposphere. Satellite measurements of HCHO columns offer "top-down" constraints to NMVOC emissions with a high spatial and temporal resolution, and can be used to validate AVOC emissions (Palmer et al., 2003; Fu et al., 2007). The retrieved satellite measurements of HCHO columns were obtained from the Global Ozone Monitoring Experiment-2 (GOME-2), and the data analysis is available in De Smedt et al. (2008).

2.2. *Source emissions*

There are several AVOC emissions inventories in the East Asian region (Tonooka et al., 2001; Klimont et al., 2002; Streets et al., 2003; Ohara et al., 2007; Bo et al., 2008; Wei et al., 2008; Zhang et al., 2009), but the INTEX-B emissions inventory from Zhang et al. (2009) is the most widely used (Lu et al., 2010; Wang et al., 2010; Zhao et al., 2010; An et al., 2013; Li et al., 2014; Tang et al., 2014). This inventory was based on the year 2006/2007, corresponding to our study period, and so we chose the emissions inventory of Zhang et al. (2009) for AVOC emissions in our work (Fig. 1b). Ammonia (NH_3) and biomass-burning emissions were provided by Streets et al. (2003). Biogenic emissions were calculated based on a global biogenic emission model, MEGAN (Guenther et al., 2006). The biological VOC (BVOC) emissions are

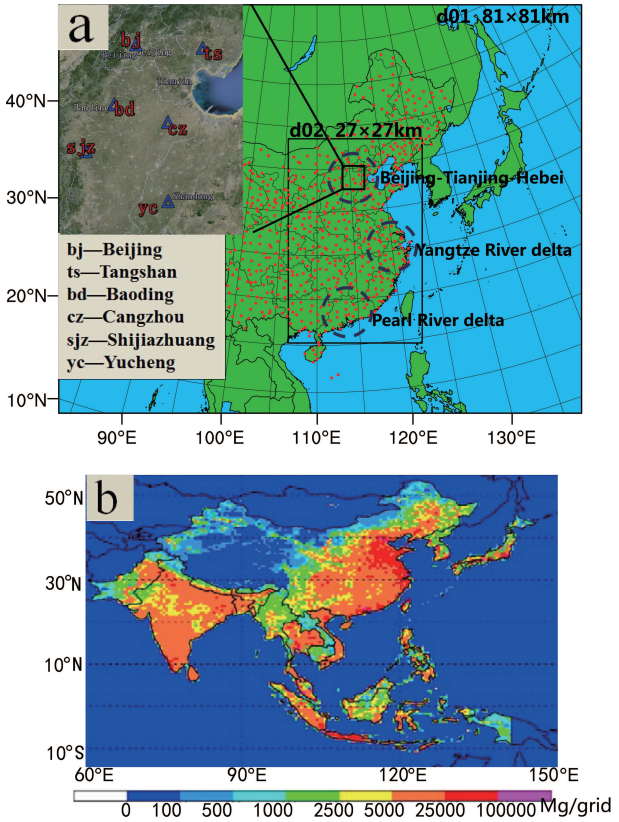

Fig. 1. (a) The domains used and the locations of the meteorological (red dots) and pollutant (blue triangles) monitoring stations; (b) the spatial distribution of AVOC emissions in Asia with a resolution of 0.5° (units: Mg grid^{-1} yr^{-1}) (Zhang et al., 2009).

quite reasonable (Palmer et al., 2006; Geng et al., 2011; Zare et al., 2012), and our sensitivity experiments demonstrated that the uncertainties of BVOC emissions were relatively minor in the studied domain with a horizontal resolution of $\geqslant 27$ km (Fig. s1) when calculated from the MEGAN model. In our study, we focused on the uncertainty of AVOC emissions.

2.3. *Model setup*

The WRF-Chem model, version 3.2.1 (Grell et al., 2005; Fast et al., 2006), was utilized in this study. The parameterization schemes used in this study are listed in Table 1. For gas chemistry, the Carbon-Bond Z (CBM-Z) mechanism (Zaveri and Peters, 1999) was used. Some additional modeled variables [$P(O_3)$, RO_x production and loss rates etc.] were saved every one hour. The Fast-J photolysis scheme was adopted to integrate instant hydrometeors, aerosols, and clouds to calculate the photolysis rates of the photochemical reactions (Fast et al., 2006). The chosen aerosol module was the MOdel for Simulating Aerosol Interactions and Chemistry (MOSAIC) (Zaveri et al., 2008), and we followed Li et al. (2011).

The domains used are shown in Fig. 1a. Domain 1 covered most areas of East Asia with a horizontal resolution of 81 km and 83×65 horizontal grid cells. Domain 2 covered the BTH, YRD and PRD, and contained 64×97 horizontal grid cells with a horizontal resolution of 27 km. We used 28 vertical model layers from the ground to 50 hPa, with the first layer ~ 30 m above the ground. Initial and boundary meteorological conditions were obtained from NCEP reanalysis data every 6 h. Chemical initial and boundary conditions were constrained by the output of the Model for OZone And Related chemical Tracers, version 4 (MOZART-4) (Emmons et al., 2010), every 6 h.

Table 1. WRF-Chem model configuration.

Options	WRF-Chem
Advection scheme	Runge–Kutta 3rd order
Cloud microphysics	Lin et al. (1983)
Long-wave radiation	RRTM
Short-wave radiation	Goddard
Surface layer	Monin–Obukhov
Land-surface model	Noah
Boundary layer scheme	YSU
Cumulus parameterization	New Grell scheme
Photolysis scheme	Fast et al. (2006)
Chemistry option	CBM-Z
Aerosol option	MOZAIC

Three model simulations of each year (2006 and 2007), denoted as S1, S2 and S3, were respectively conducted to evaluate the impacts of the uncertainty in AVOC emissions on the RO_x budget and $P(O_3)$ in the BTH, YRD, and PRD. S1 used the emissions mentioned above, and then a 68% increase and a 68% decrease were respectively utilized in S2 and S3 according to the uncertainty range given by Zhang et al. (2009). The same percentage changes were applied to each of the AVOC species for each simulation (i.e., S2 and S3) due to very limited information and scarce measurements of AVOC emission intensities in China. A spin-up period of seven days was used for each simulation.

3. Results and discussion

3.1. *Evaluation of model performance*

3.1.1. *Comparison of simulated and observed meteorological factors*

The statistical metrics used for model evaluation were mean bias (MB), mean error (ME), root-mean-square error (RMSE), normalized mean bias (NMB), normalized mean error (NME), index of agreement (IOA), and correlation coefficient (CC). Their definitions are available in Simon et al. (2012). The RMSE was 2.5°C for TA, 16.3% for RH, 2.5 m s^{-1} for WS, and 99.3° for WD, whereas the IOA was 0.90 for TA, 0.78 for RH, 0.56 for WS, and 0.65 for WD (Table 2). These statistical metrics indicated that the simulations of TA and RH were much better than those of WS and WD. The results were very similar to the studies of Wang et al. (2010) and Li et al. (2012) using the fifth-generation Pennsylvania State University/National Center for Atmospheric Research Mesoscale Model (MM5), and those of Zhang et al. (2012) using the WRF model (Table 2).

3.1.2. *Comparison of simulations and observations of O_3, NO_2, RO_x, and HCHO*

The WRF-Chem model (an emission-based model) simulated the O_3 observations well at six stations in the BTH (Fig. 2a), with a CC of 0.84, NMB of −4.0%, NME of 35.0%, and IOA of 0.91 (Table 3), better than the results of Li et al. (2012) and Wang et al. (2010). The model results for daily variations of NO_2 considerably overestimated the observations at the Baoding and Yucheng stations in most cases (Fig. 2b). This overestimation could be related to the uncertainty of emissions. The NO_2 simulations were comparable with those of Wang et al. (2010) and Li et al. (2012) using the Commu-

Table 2. Performance metrics of WRF-Chem meteorology simulations in August 2007.

Temperature (°C)			Relative Humidity (%)			Wind Speed (m s^{-1})			Wind direction (°)			
RMSE	MB	IOA	RMSE	MB	IOA	RMSE	MB	IOA	RMSE	MB	IOA	Reference
2.5	0.2	0.90	16.3	−5.5	0.78	2.5	1.6	0.56	99.3	2.6	0.65	This work
	−0.9	0.90		−1.3	0.78	2.1	0.9	0.65		2.5		Wang et al. (2010)
	0.5	0.88		−1.1	0.86	1.5	0.6	0.62		2.6		Li et al. (2012)
3.1	0.8		17.4	−5.7		2.2	1.1		60.9	8.2		Zhang et al. (2012)

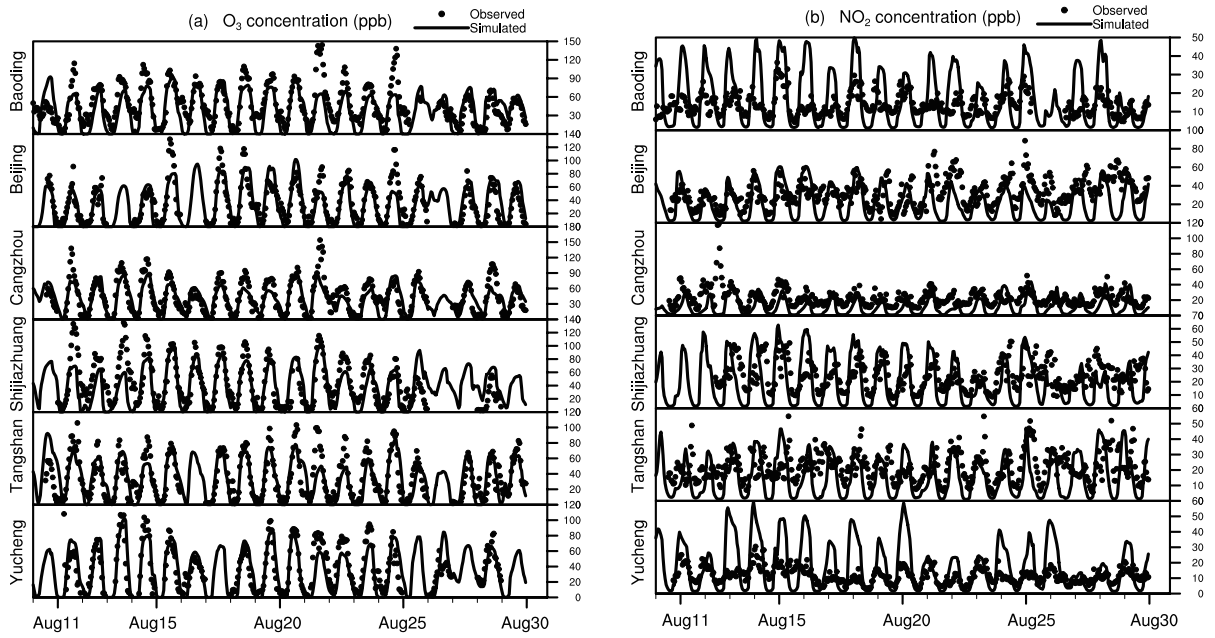

Fig. 2. Time series of simulated and observed concentrations of (a) O_3 and (b) NO_2 near the ground at six stations of the BTH in August 2007.

Table 3. Performance metrics of WRF-Chem simulations of O_3 and NO_2 in August 2007.

Variables	MB (ppb)	ME (ppb)	RMSE (ppb)	NMB (%)	NME (%)	IOA	CC	Reference
O_3	−1.4	12.0	16.6	−4.0	35.0	0.91	0.84	This work[a]
				−5.4	37.1		0.73	Wang et al. (2010)
				30.2	55.8	0.91	0.78	Li et al. (2012)[b]
NO_2	−10.9	16.5	20.5	−33.0	50.0	0.61	0.43	This work[a]
				−26.8	52.1		0.52	Wang et al. (2010)
				13.8	48.4	0.91	0.53	Li et al. (2012)[b]

[a]Metrics were calculated based on the observations at six stations of the BTH.
[b]Model used was CMAQ.

nity Multi-scale Air Quality Model (CMAQ), with an NMB of −33.0%, NME of 50.0%, IOA of 0.61, and CC of 0.43, respectively (Table 3).

Diurnal variations of OH were simulated well (Fig. 3 for case S1) at the Guangzhou Backgarden site of the PRD, with a CC of 0.81, IOA of 0.91, NME of 40.9%, and RMSE of 3×10^6 molecules cm^{-3} (Table 4). Diurnal fluctuations of HO_2 were well captured (Fig. 3 for case S1), with a CC of 0.82 (Table 4); however, HO_2 peaks were substantially underestimated (Fig. 3 for case S1; Table 4). This underestimation was associated with the underestimated NMVOC emissions, because a 68% increase in the AVOC emissions led to significant improvements in the HO_2 simulations at the Guangzhou Backgarden site of the PRD (Fig. 3 for case S2). The peak time of OH and HO_2 was varied with changes in AVOC emissions (Fig. 3). The reason is that 68% of increases (case S2) or decreases (case S3) in AVOC emissions led to obvious changes in the maximum production rates for OH and HO_2 dominant sources (Fig. s7). During 20–21 July, the strong wind lasted for $\sim$ 8 hours (Fig. s8) and was favorable for dilution and long-range transport of pollutants, and dwarfed the role of changes in local AVOC emissions, so the simulated OH indicated almost no difference for the three cases (Fig. 3).

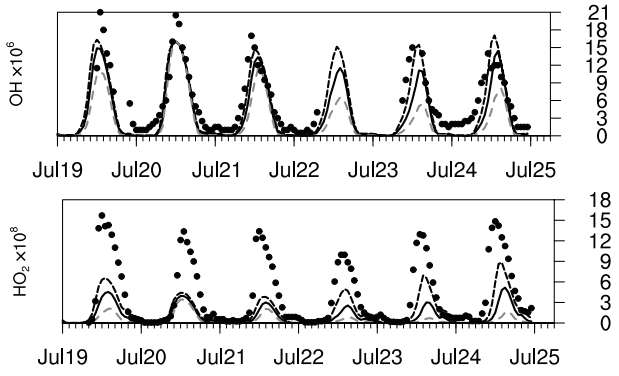

Fig. 3. Time series of hourly mean simulations of OH and HO_2 (molecules cm^{-3}) for cases S1(solid lines), S2(black dash lines) and S3(grey dash lines) and the corresponding measurements from Lu et al. (2012)(solid dots) at the Guangzhou Backgarden site of the PRD in July 2006.

Table 4. Performance metrics of WRF-Chem simulations of OH and HO_2 radicals in July 2006. Observations were from Lu et al. (2012). The units of OH and its MB, ME, and RMSE are $\times 10^6$ molecules cm^{-3}, while those of HO_2 and its MB, ME, and RMSE are $\times 10^8$ molecules cm^{-3}.

Radicals	MB	ME	RMSE	NMB (%)	NME (%)	IOA	CC
OH	−1.9	2.3	3.0	−34.6	40.9	0.91	0.81
HO_2	−3.0	3.0	4.7	−75.8	75.9	0.58	0.82

Vertically, the maximum concentrations of OH and HO_2 appeared at $\sim$ 1 km above the ground (Fig. s6), consistent with the results of Ma et al. (2012), who calculated their results using an observation-based model constrained by measured daytime mean trace gas and aerosol concentrations. Although emission-based models (e.g., the WRF-Chem model used in this study) depend significantly on the accuracy of pollutant source emissions, whereas observation-based models rely on observed trace gas concentrations, both simulations are comparable when the source emissions are accurate in the same studied period.

The correlations between monthly GOME-2 and simulated HCHO columns in both urban (Fig. 4a) and suburban (Fig. 4b) areas in domain 2 in August 2007 also demonstrated that the satellite observations were 30% (18%) higher than the simulations in urban (suburban) areas. A 68% increase in AVOC emissions produced a nice agreement with the observations in suburban areas (Fig. 4b), and a noticeable improvement in the simulations in urban areas, although the observations were still $\sim$ 15% higher than the corresponding simulations (Fig. 4a). The above results indicated that the AVOC emissions were underestimated by $\sim$ 68% in suburban areas and by more than 68% in urban areas. For monthly diurnal averages in Beijing of the BTH, the simulated OH peak was 14.4×10^6 molecules cm^{-3} (Fig. 5), which was $\sim$ 60% higher than the 9×10^6 molecules cm^{-3} simulated by Liu et al. (2012) with an observation-based model constrained by measured CO, O_3, NO, HONO, hydrocarbons (C_2–C_9), formaldehyde (HCHO), acetaldehyde (ALD2), acetone, and aerosol surface areas in the first model layer. The simulated maxima of HO_2 and RO_2 were 5.3×10^8 molecules cm^{-3} and 3.1×10^8 molecules cm^{-3} (Fig. 5), respectively, comparable with the 6.8×10^8 molecules cm^{-3} and 4.5×10^8 molecules cm^{-3}, respectively, reported by Liu et al. (2012).

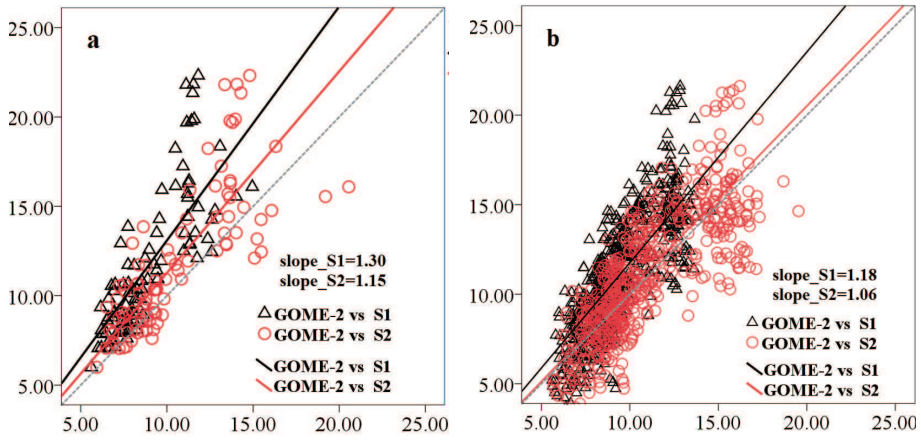

Fig. 4. HCHO columns ($\times 10^{15}$ molec cm^{-2}) observed by GOME-2 versus those simulated by the WRF-chem model at (a) 94 urban and (b) 584 suburban sites in domain 2 in August 2007. The black and red lines indicate the linear regression slopes for cases S1 and S2, respectively.

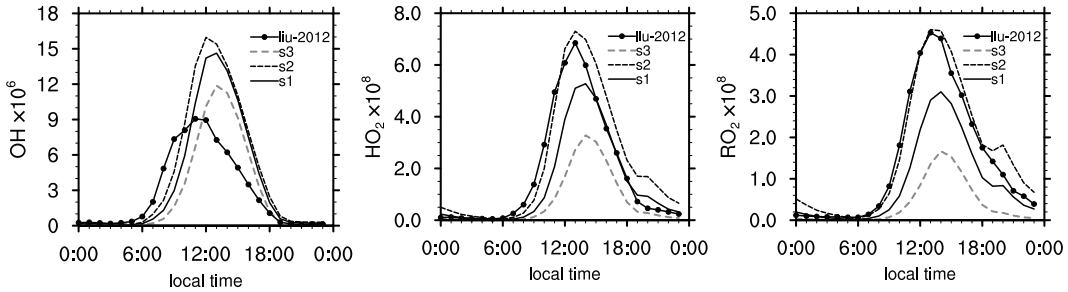

Fig. 5. Comparison of the simulated monthly mean diurnal profiles of OH, HO_2 and RO_2 (molecules cm^{-3}) for cases S1, S2, and S3 with those of Liu et al. (2012) in Beijing in July 2006.

3.2. *RO_x budgets*

Three major cities (Beijing, Shanghai, and Guangzhou), were chosen to respectively represent the typical urban sites of the BTH, YRD, and PRD for examination of production/loss rates of OH [P(OH)/L(OH)], HO_2 [$P(HO_2)$/$L(HO_2)$], and RO_2 [$P(RO_2)$/$L(RO_2)$]. P(OH) was dominated by the rate of NO + HO_2 in Beijing (80%), Shanghai (69%), and Guangzhou (73%) for case S1; whereas, the predominant $P(HO_2)$ was from CO + OH (44% in Beijing, 32% in Shanghai, and 36% in Guangzhou), CH_3O_2 + NO (16% in Beijing, 18% in Shanghai, and 16% in Guangzhou), HCHO + OH (11% in Beijing, 10% in Shanghai, and 11% in Guangzhou), and ISOPRAD (lumped peroxyradical of isoprene) + NO (7% in Beijing, 11% in Shanghai, and 17% in Guangzhou) (not shown). The reactions of ISOP (isoprene), ETH (ethene), CH_4, C_2H_6, OLET (terminal olefin carbons C=C), OLEI (internal olefin carbons C=C), ALD2, MGLY (methylglyoxal), and XYL (xylene) with OH were the major $P(RO_2)$ sources, accounting for 82% in Beijing, 85% in Shanghai, and 90% in Guangzhou (not shown). The dominant L(OH) was from CO + OH (37% in Beijing, 24% in Shanghai, and 30% in Guangzhou), NO_2 + OH (20% in Beijing, 30% in Shanghai, and 23% in Guangzhou), and ISOP + OH only for Guangzhou (16%); whereas, $L(HO_2)$ was dominated by the reaction of NO + HO_2 (93%–98%), and $L(RO_2)$ was dominated by the reaction of NO + CH_3O_2 (86%–94%) for all the three cities (not shown), where NO_x emissions are high (Zhang et al., 2009).

The total primary RO_x production rates were 2.07 ppbv h^{-1} in Beijing (1.23 ppbv h^{-1} for OH, 0.51 ppbv h^{-1} for HO_2, and 0.33 ppbv h^{-1} for RO_2) (Fig. 6a), 1.53 ppbv h^{-1} in Shanghai (1.02 ppbv h^{-1} for OH, 0.26 ppbv h^{-1} for HO_2, and 0.25 ppbv h^{-1} for RO_2), and 1.50 ppbv h^{-1} in Guangzhou (1.07 ppbv h^{-1} for OH, 0.23 ppbv h^{-1} for HO_2, and 0.20 ppbv h^{-1} for RO_2), respectively. The two largest contributors to the total RO_x production rate were the reaction of O^1D + H_2O (0.81 ppbv h^{-1} in Beijing, 0.56 ppbv h^{-1} in Shanghai, and 0.74 ppbv h^{-1} in Guangzhou), and photolysis of HCHO, ALD2, MGLY, acetone, and others (0.64 ppbv h^{-1} in Beijing, 0.38 ppbv h^{-1} in Shanghai, and 0.33 ppbv h^{-1} in Guangzhou). A 68% increase in AVOC emissions (case S2) yielded a significant enhancement in the total primary RO_x production: 3.06 ppbv h^{-1} (48%) in Beijing (Fig. 6b), 2.17 ppbv h^{-1} (42%) in Shanghai, and 2.03 ppbv h^{-1} (35%) in Guangzhou. These values were lower than those in Mexico City in 2006 (4.75 ppbv h^{-1}; Dusanter et al., 2009), and Birmingham, UK (4.5 ppbv h^{-1}; Emmerson et al., 2005). On the contrary, a 68% decrease in AVOC emissions (case S3) produced a noticeable reduction in the total primary RO_x production: 1.27 ppbv h^{-1} (39%) in Beijing, 1.03 ppbv h^{-1} (32%) in Shanghai, and 1.11 ppbv h^{-1} (26%) in Guangzhou.

RO_x radicals are ultimately scavenged from the atmosphere through dry and wet deposition of radical reservoir species (e.g., HNO_3 and organic acids). The net radical losses via NO_x–radical reactions were 0.87 ppbv h^{-1} to 1.40 ppbv h^{-1}, including NO_2 + OH → HNO_3 [1.24 ppbv h^{-1} in Beijing (Fig. 6a), 0.87 ppbv h^{-1} in Shanghai, and 0.84 ppbv h^{-1} in Guangzhou]. The net radical losses via NO_x–radical reactions were much larger than those via radical–radical reactions [0.22 ppbv h^{-1} in Beijing (Fig. 6a), 0.08 ppbv h^{-1} in Shanghai, and 0.11 ppbv h^{-1} in Guangzhou], indicating a feature of chemistry in NO_x-rich urban environments. A 68% increase in AVOC emissions (case S2) led to substantial losses of RO_x radicals, e.g., the net radical losses via NO_x–radical reactions were respectively enhanced by 33% (1.86 ppbv h^{-1}) in Beijing (Fig. 6b), by 32% (1.16 ppbv h^{-1}) in Shanghai, and by 20% (1.04 ppbv h^{-1}) in Guangzhou; whereas, those via radical–radical reactions were respectively increased by 118% (0.48 ppbv h^{-1}) in Beijing (Fig. 6b), by 88% (0.15 ppbv h^{-1}) in Shanghai, and by 91% (0.21 ppbv h^{-1}) in Guangzhou. On the contrary, a 68% decrease in AVOC emissions (case S3) reduced the net radical losses via NO_x–radical reactions by 15%–29% and decreased those via radical–radical reactions by 36%–68 % in the three

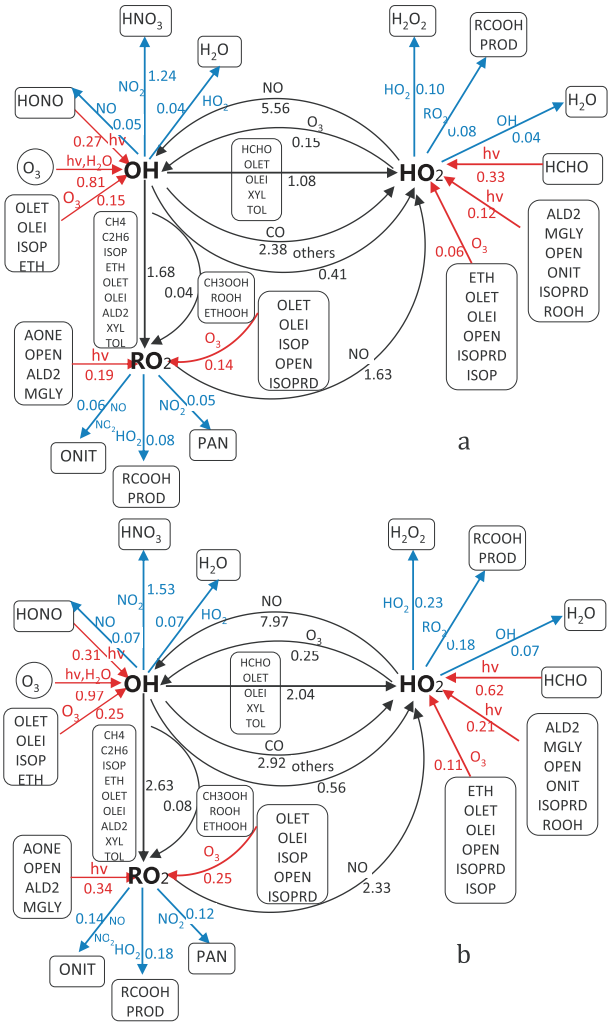

Fig. 6. Daytime average budgets of RO_x radicals in Beijing in August 2007 for cases (a) S1 and (b) S2. Primary RO_x sources and sinks are marked in red and blue, respectively. The production and loss rates are in units of ppbv h^{-1}.

cities.

3.3. *Ozone production rate*

The ozone production rate [$P(O_3)$] and loss rate [$L(O_3)$] can be defined as (Kanaya et al., 2009):

$P(O_3) = [NO](K_{HO_2+NO}\,[HO_2] + K_{CH_3O_2+NO}\,[CH_3O_2] + K_{RO_2+NO}\,[RO_2] + K_{othersR+NO}\,[othersR])$,

$L(O_3) = K_{O^1D+H_2O}\,[O^1D][H_2O] + [O_3](K_{OH+O_3}\,[OH] + K_{HO_2+O_3}\,[HO_2] + K_{VOCs+O_3}\,[VOCs])$,

where othersR denotes other radicals [e.g., C_2O_3 (peroxyacyl radical) and CRO (methylphenoxy radical)]. Daily variations of $P(O_3)$ were well simulated at the urban [PKU (39.99°N, 116.30°E)] and suburban [YUFA (39.51°N, 116.30°E)] stations in Beijing by the WRF-Chem model (Fig. 7, case S1), compared with those simulated by Lu et al. (2010) using an observation-based model constrained by measurements of O_3, NO, HONO, CO, hydrocarbons (C_3–C_{12}), photolysis frequencies, H_2O, air temperature and pressure. However, our simulations substantially underestimated the $P(O_3)$ peaks in most cases, particularly at the PKU station (Fig. 7, case S1). When the AVOC emissions were increased by 68%, the $P(O_3)$ peaks were significantly improved (13%–82%), especially at the YUFA station (Fig. 7, case S2), but the simulated peaks of $P(O_3)$ at the PKU station were still much lower than those of Lu et al. (2010). The improvements in the simulated peaks of $P(O_3)$ ascribed to those of HO_2 and RO_2 were caused by a 68% increase in AVOC emissions (Fig. 5, case S2). Decreases in the AVOC emissions lowered the concentrations of HO_2 and RO_2 considerably (Fig. 5, case S3), leading to substantial underestimation of the $P(O_3)$ peaks (13%–69%) (Fig. 7, case S3). The contrast between cases S2 and S3 further demonstrated that the AVOC emissions in the BTH in 2006/2007 were significantly underestimated (i.e., $\sim$ 68% in suburban areas and larger than 68% in urban areas). For the PRD, a 68% increase in the AVOC emissions significantly improved the simulated HO_2 peaks (Fig. 3, case S2), resulting in an 8%–70% increase in the $P(O_3)$ peaks for case S2; whereas, 68% decreases in the AVOC emissions lowered the HO_2 peaks substantially, and reduced the $P(O_3)$ peaks by 6%–63% for case S3 (not shown). Similarly, large increases (decreases) in the AVOC emissions yielded 15%–85% (12%–65%) enhancements (reductions) in the $P(O_3)$ peaks in the YRD for case S2 (S3) (not shown).

Figure 8 shows the monthly average diurnal profiles of $P(O_3)$ and $L(O_3)$ in Beijing in August 2007. The monthly average diurnal maxima of $P(O_3)$ and $L(O_3)$ were 15.9 ppbv h^{-1} and 1.7 ppbv h^{-1}, respectively. The results were comparable with the simulations of Kanaya et al. (2009) [i.e., 13.6 ppbv h^{-1} for $P(O_3)$ and 2.0 ppbv h^{-1} for $L(O_3)$ at Mount Tai in June of 2006], but our simulation of $P(O_3)$ was much lower than the simulations of Lu et al. (2010) (i.e., 69.5 ppbv h^{-1} at the PKU station and 25.8 ppbv h^{-1} at the YUFA station in August 2006). When the AVOC emissions were enhanced/reduced by 68%, the $P(O_3)$ peak was increased/decreased by 22.5 ppbv h^{-1} (42%)/9.5 ppbv h^{-1} (40%), and the $L(O_3)$ maximum was increased/decreased to 2.3 ppbv h^{-1} (35%)/1.2 ppbv h^{-1} (29%). The $P(O_3)$ peak for case S2 was much closer to the simulation of Lu et al. (2010) at the YUFA station, further indicating that the AVOC emissions in suburban areas of the BTH in 2006/2007 were underestimated by $\sim$ 68%. The average daytime peak of $P(O_3)$ occurred at $\sim$ 1100 LST (Fig. 8, case S2), earlier than the peaks of RO_x at $\sim$ 1300 LST (Fig. 5, case S2), because the NO concentrations were decreased from morning to early afternoon, consistent with results in Mexico City (Shirley et al., 2006) and Beijing (Liu et al., 2012).

In the three regions, the predominant contribution to $P(O_3)$ was the reaction of HO_2 + NO, accounting for 68% in Beijing, 66% in Shanghai, and 65% in Guangzhou (Fig. 9). The major contribution to $L(O_3)$ was the reactions of O^1D + H_2O (47%), HO_2 + O_3 (17%), OH + O_3 (16%), and OLET + O_3 (16%) in Beijing, the reactions of O^1D + H_2O (70%) and OLET + O_3 (16%) in Shanghai, and the reactions of O^1D + H_2O (67%) and OH + O_3 (13%) in Guangzhou (Fig. 9). Sixty-eight percent increases (decreases) in AVOC emissions reduced (enhanced) the $P(O_3)$ via the reaction of HO_2 + NO

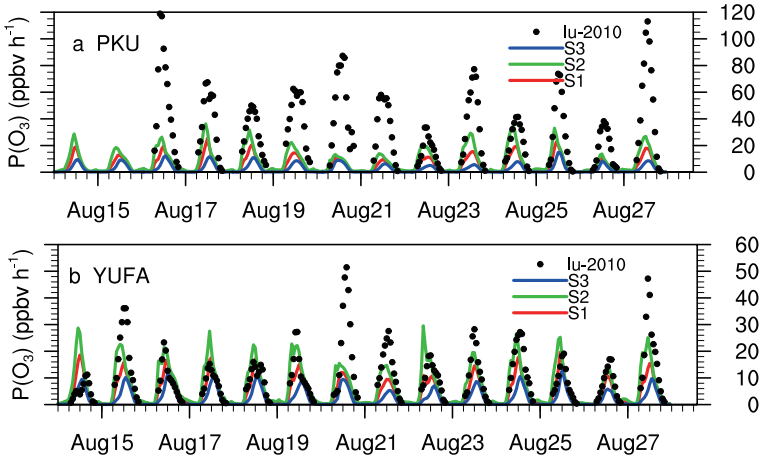

Fig. 7. Comparison of hourly simulations of $P(O_3)$ for cases S1, S2 and S3 with those of Lu et al. (2010) at the PKU and YUFA stations of Beijing in August 2006.

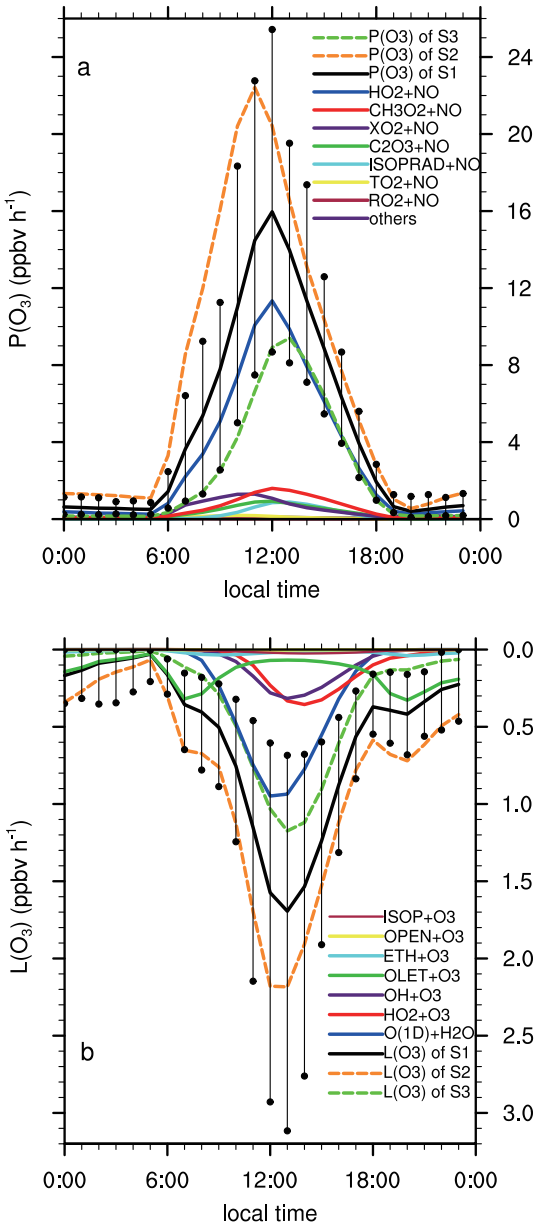

Fig. 8. Monthly average diurnal profiles of O_3 (a) production and (b) loss rates calculated with the WRF-Chem model in Beijing in August 2007. The vertical bars denote monthly standard deviations, and black dots denote the maximum and minimum deviations.

by 65% (73%) in Beijing, by 63% (71%) in Shanghai, and by 64% (68%) in Guangzhou (Fig. 9, cases S2 and S3). The $L(O_3)$ was decreased via the reaction of $O^1D + H_2O$ by 40% in Beijing and by 62% in Shanghai, increased via the reaction of OLET + O_3 by 20% in Beijing and by 22% in Shanghai, and reduced via the reaction of $O^1D + H_2O$ by 62% in Guangzhou due to 68% increases in AVOC emissions (case S2) (Fig. 9). On the contrary, 68% decreases in the AVOC emissions (case S3) led to a 60% increase of the $L(O_3)$ in Beijing, an 81% increase in Shanghai, and a 73% increase in Guangzhou, via the reaction of $O^1D + H_2O$ (Fig. 9).

3.4. *Implications for underestimation of AVOC emissions*

A 68% increase in AVOC emissions respectively enhanced monthly meridional-mean daytime (0600–1800 LST) concentrations of OH, HO_2, and RO_2 by 1%–5% within 150 m above the ground (Fig. 10a), and by 4%–16% (Fig. 10b) and 6%–26% (Fig. 10c) in the atmospheric boundary layer (ABL, $\sim$ 1 km above the ground), respectively; whereas, a 68% decrease in AVOC emissions reduced the monthly meridional-mean daytime concentrations of OH, HO_2, and RO_2 by 2%–8% within 150 m above the ground (Fig. 10d), and by 6%–15% (Fig. 10e) and 8%–24% (Fig. 10f) in the ABL, respectively.

A 68% increase in AVOC emissions enhanced monthly-mean daytime concentrations (MDCs) of OH by 4%–48%, 4%–52%, and 4%–44% in the BTH, YRD and YRD, respectively (Table 5). The MDCs of HO_2 were respectively enhanced by 10%–120%, 10%–140%, and 10%–120% in the BTH, YRD and YRD (Table 5). For the MDCs of RO_2, a 68% increase in AVOC emissions led to a 20%–280% increase in the BTH, a 20%–240% increase in the YRD, and a 10%–140% increase in the PRD (Table 5). Remarkable enhancements of OH, HO_2, and RO_2 due to the notable increases in AVOC emissions demonstrated that NO_x and water vapor were relatively abundant and O_3 concentrations were high in the BTH, YRD, and PRD (Fig. s3).

When AVOC emissions were increased by 68%, the MDCs of SO_4^{2-}, NO_3^-, NH_4^+, and $PM_{2.5}$ were respectively enhanced by 2%–16%, 2%–20%, 2%–20%, and 1%–16% in the BTH, YRD and PRD (Table 5), implying that daily and hourly concentrations of secondary organic aerosols could be substantially underestimated when AVOCs emissions were underestimated by 68%, and remarkable underestimation of daily and hourly concentrations of organic and inorganic aerosols could underestimate cloud condensation nuclei and overestimate local and regional radiation.

The Ln/Q ratio for judging O_3–NO_x–VOCs sensitivity has been extensively used (Sillman and He, 2002; Kleinman, 2005; Song et al., 2012), where Ln denotes radical termination by NO_x, and Q represents radical production. If Ln/Q > 0.5, then the photochemistry is VOC-sensitive; if Ln/Q < 0.5, then it is NO_x-sensitive. We calculated the Ln/Q ratios and found that the Ln/Q ratios in most large cities in the three regions were > 0.5 (Fig. s4d), indicating these areas were

Table 5. Percentage enhancements of OH, HO_2, RO_2, SO_4^{2-}, NO_3^-, NH_4^+, and $PM_{2.5}$ due to a 68% increase in AVOC emissions in the BTH, YRD and PRD in August 2007.

Species	BTH	YRD	PRD
OH	4–48	4–52	4–44
HO_2	10–120	10–140	10–120
RO_2	20–280	20–240	10–140
SO_4^{2-}	2–10	4–16	4–10
NO_3^-	2–20	4–20	4–18
NH_4^+	2–14	2–20	4–16
$PM_{2.5}$	1–8	2–16	4–12

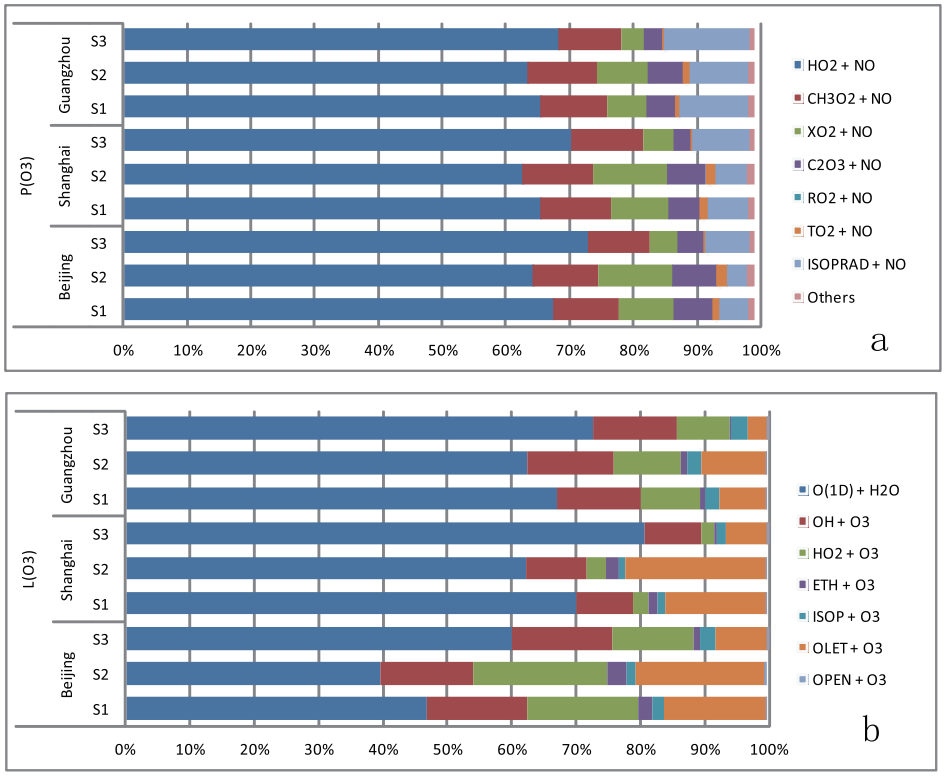

Fig. 9. Daytime average fractional contributions to the major O_3 (a) production and (b) loss rates in Beijing, Shanghai and Guangzhou in August 2007 for cases S1, S2 and S3.

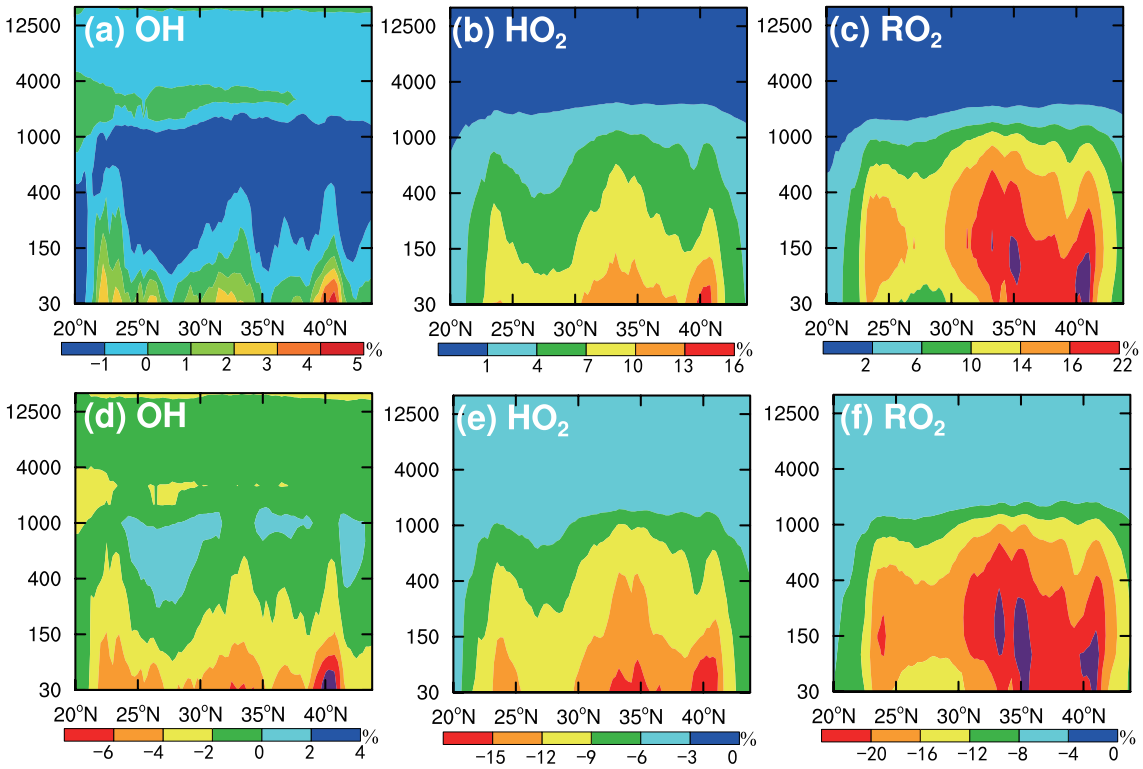

Fig. 10. Monthly meridional-mean daytime (0600–1800 LST) enhancements of (a) OH, (b) HO_2, and (c) RO_2, and decreases of (d) OH, (e) HO_2, and (f) RO_2 as a function of latitude and altitude in domain 2 in August 2007 due to a 68% increase or decrease in AVOC emissions.

VOC-sensitive, consistent with other studies (Shao et al., 2009; Lu et al., 2010). A 68% increase in AVOC emissions led to a chemical regime change [from a VOC-sensitive regime ($Ln/Q > 0.5$) to a NO_x-sensitive regime ($Ln/Q < 0.5$)] in some areas, especially around the megacities (Fig. s4e), suggesting that the VOC-sensitive areas could be enlarged when O_3 control measures were based on the AVOC emissions of Zhang et al. (2009).

4. Conclusions

Diagnostic variables were incorporated into the WRF-Chem model to quantify the effect of the uncertainty in AVOC emissions on the RO_x budget and $P(O_3)$ in the three most rapidly-developing economic growth regions of China (i.e., the BTH, YRD, and PRD). Results showed that a 68% increase (decrease) in the AVOC emissions led to 4%–52% increases (2%–36% decreases) of OH, 10%–140% increases (4%–60% decreases) of HO_2, and 10%–280% increases (5%–80% decreases) of RO_2 in the BTH, YRD, and PRD. For three typical urban cities (Beijing, Shanghai, and Guangzhou) in the BTH, YRD, and PRD, the total primary RO_x production rate near the ground was 1.50 ppbv h^{-1} to 2.07 ppbv h^{-1}; the two largest contributors to the total RO_x production rate were the reaction of $O^1D + H_2O$ (0.56 ppbv h^{-1} to 0.81 ppbv h^{-1}), and photolysis of HCHO, ALD2, MGLY, acetone, and others (0.33 ppbv h^{-1} to 0.64 ppbv h^{-1}); the major RO_x sink was via the reaction of $OH + NO_2$ (71%–85%); the major contributor to $P(O_3)$ was the reaction of HO_2+ NO (65%–68%); and the dominant contributor to $L(O_3)$ was the reaction of $O^1D + H_2O$ (47%–70%).

A 68% increase (decrease) in the AVOC emissions enhanced (reduced) the total primary RO_x production by 48% (39%) in Beijing, 42% (32%) in Shanghai, and 35% (26%) in Guangzhou. When the AVOC emissions were increased (decreased) by 68%, the $P(O_3)$ was reduced (enhanced) by $\sim$ 65% (68%–73%) via the reaction of HO_2 + NO, and the $L(O_3)$ was reduced (enhanced) by 40%–62% (60%–81%) via the reaction of $O^1D + H_2O$ in the three cities. Comparison of our simulations with satellite HCHO observations, ground measurements of OH and HO_2, as well as the simulated $P(O_3)$ with an observation-based model demonstrated that AVOC emissions in 2006 from Zhang et al. (2009) were underestimated by $\sim$ 68% in suburban areas and by more than 68% in urban areas. Substantial underestimation of AVOC emissions could considerably underestimate daily and hourly concentrations of secondary organic aerosols and inorganic aerosols, underestimate cloud condensation nuclei and local and regional radiation, and enlarge the VOC-sensitive areas.

Acknowledgements. This research was partially supported by the National Natural Science Foundation of China (Grant Nos. 41175105 and 41105098), the Beijing Natural Science Foundation (Grant No. 8144054), a Key Project of CAS (Grant No. XDB05030301), and the Carbon and Nitrogen Cycle Project of IAP, CAS. Special thanks are given to Prof. WANG Yuesi from IAP, CAS, for offering observed data of NO_x and O_3 in the Beijing–Tianjin–Hebei region. Many thanks are extended to the two anonymous reviewers for their key suggestions.

Electronic supplementary material: Supplementary material is available in the online version of this article at http://dx.doi.org/10.1007/s00376-014-3251-z.

REFERENCES

An, J. L., 2006: Ozone production efficiency in Beijing area with high NO_x emissions. *Acta Scientiae Circumstantiae*, **26**, 652–657.

An, J. L., Y. Li, Y. Chen, J. Li, Y. Qu, and Y. J. Tang, 2013: Enhancements of major aerosol components due to additional HONO sources in the North China Plain and implications for visibility and haze. *Adv. Atmos. Sci.*, **30**, 57–66.

Avery, R. J., 2006: Reactivity-based VOC control for solvent products: More efficient ozone reduction strategies. *Environmental Science and Technology*, **40**, 4845–4850.

Bo, Y., H. Cai, and S. D. Xie, 2008: Spatial and temporal variation of historical anthropogenic NMVOCs emission inventories in China. *Atmos. Chem. Phys.*, **8**, 7297–7316.

Carter, W. P., 1994: Development of ozone reactivity scales for volatile organic compounds. *Journal of the Air and Waste Management Association*, **44**, 881–899.

Chameides, W., and Coauthors, 1992: Ozone precursor relationships in the ambient atmosphere. *J. Geophys. Res.*, **97**, 6037–6055.

Chen, S., and W. H. Brune, 2012: Global sensitivity analysis of ozone production and O_3-NO_x-VOC limitation based on field data. *Atmos. Environ.*, **55**, 288–296.

Chou, C. C. K., C.-Y. Tsai, C.-J. Shiu, S. C. Liu, and T. Zhu, 2009: Measurement of NO_y during Campaign of Air Quality Research in Beijing 2006 (CAREBeijing-2006): Implications for the ozone production efficiency of NO_x. *J. Geophys. Res.*, **114**, D00G01, doi: 10.1029/2008jd010446.

De Smedt, I., J. F. Müller, T. Stavrakou, R. van der A, H. Eskes, and M. Van Roozendael, 2008: Twelve years of global observations of formaldehyde in the troposphere using GOME and SCIAMACHY sensors. *Atmos. Chem. Phys.*, **8**, 4947–4963.

Dusanter, S., and Coauthors, 2009: Measurements of OH and HO2 concentrations during the MCMA-2006 field campaign–Part 2: Model comparison and radical budget. *Atmos. Chem. Phys.*, **9**, 6655–6675.

Emmerson, K. M., N. Carslaw, M. J. Pilling, 2005: Urban atmospheric chemistry during the PUMA campaign 2: Radical budgets for OH, HO2 and RO2. *Journal of Atmospheric Chemistry*, **52**, 165–183.

Emmons, L. K., and Coauthors, 2010: Description and evaluation of the Model for Ozone and Related chemical Tracers, version 4 (MOZART-4). *Geoscientific Model Development Discussions*, **3**, 43–67.

Fast, J. D., and Coauthors, 2006: Evolution of ozone, particulates, and aerosol direct radiative forcing in the vicinity of Houston using a fully coupled meteorology-chemistry-aerosol model. *J. Geophys. Res.*, **111**, D21305, doi: 10.1029/2005jd006721.

Fu, J. S., D. G. Streets, C. J. Jang, J. M. Hao, K. He, L. T. Wang, and Q. Zhang, 2009: Modeling regional/urban ozone and particulate matter in Beijing, China. *Journal of the Air and Waste Management Association*, **59**, 37–44.

Fu, T.-M., and Coauthors, 2007: Space-based formaldehyde measurements as constraints on volatile organic compound emissions in east and south Asia and implications for ozone. *J. Geophys. Res.*, **112**, D06312, doi: 10.1029/2006JD007853.

Gao, H., and Coauthors, 2011: A study of air pollution of city clusters. *Atmos. Environ.*, **45**, 3069–3077.

Geng, F., X. Tie, A. Guenther, G. Li, J. Cao, and P. Harley, 2011: Effect of isoprene emissions from major forests on ozone formation in the city of Shanghai, China. *Atmos. Chem. Phys.*, **11**, 10449–10459.

Grell, G. A., S. E. Peckham, R. Schmitz, S. A. McKeen, G. Frost, W. C. Skamarock, and B. Eder, 2005: Fully coupled "online" chemistry within the WRF model. *Atmos. Environ.*, **39**, 6957–6975.

Guenther, A., T. Karl, P. Harley, C. Wiedinmyer, P. I. Palmer, and C. Geron, 2006: Estimates of global terrestrial isoprene emissions using MEGAN (Model of Emissions of Gases and Aerosols from Nature). *Atmos. Chem. Phys.*, **6**, 3181–3210.

Hao, J., D. He, Y. Wu, L. Fu, and K. He, 2000: A study of the emission and concentration distribution of vehicular pollutants in the urban area of Beijing. *Atmos. Environ.*, **34**, 453–465.

Huang, C., and Coauthors, 2011: Emission inventory of anthropogenic air pollutants and VOC species in the Yangtze River Delta region, China. *Atmos. Chem. Phys.*, **11**, 4105–4120.

Kanaya, Y., and Coauthors, 2009: Rates and regimes of photochemical ozone production over Central East China in June 2006: A box model analysis using comprehensive measurements of ozone precursors. *Atmos. Chem. Phys.*, **9**, 7711–7723.

Kleinman, L. I., 2005: The dependence of tropospheric ozone production rate on ozone precursors. *Atmos. Environ.*, **39**, 575–586.

Kleinman, L. I., P. H. Daum, Y. N. Lee, L. J. Nunnermacker, S. R. Springston, J. Weinstein-Lloyd, and J. Rudolph, 2002: Ozone production efficiency in an urban area. *J. Geophys. Res.*, **107**, ACH 23-1–ACH 23-12, doi: 10.1029/2002JD002529.

Klimont, Z., D. G. Streets, S. Gupta, J. Cofala, L. Fu, and Y. Ichikawa, 2002: Anthropogenic emissions of non-methane volatile organic compounds in China. *Atmos. Environ.*, **36**, 1309–1322.

Li, L., and Coauthors, 2012: Process analysis of regional ozone formation over the Yangtze River Delta, China using the Community Multi-scale Air Quality modeling system. *Atmos. Chem. Phys.*, **12**, 10 971–10 987.

Li, Y., J. An, M. Min, W. Zhang, F. Wang, and P. Xie, 2011: Impacts of HONO sources on the air quality in Beijing, Tianjin and Hebei Province of China. *Atmos. Environ.*, **45**, 4735–4744.

Li, Y., J. An, and I. Gultepe, 2014: Effects of additional HONO sources on visibility over the North China Plain. *Adv. Atmos. Sci.*, **31**(5), 1221–1232, doi: 10.1007/s00376-014-4019-1.

Liu, X.-H., and Coauthors, 2010: Understanding of regional air pollution over China using CMAQ, Part I: Performance evaluation and seasonal variation. *Atmos. Environ.*, **44**, 2415–2426.

Liu, Z., and Coauthors, 2012: Summertime photochemistry during CAREBeijing-2007: RO_x budgets and O_3 formation. *Atmos. Chem. Phys.*, **12**, 7737–7752.

Lu, K., and Coauthors, 2010: Oxidant (O_3 + NO_2) production processes and formation regimes in Beijing. *J. Geophys. Res.*, **115**, D07303.

Lu, K. D., and Coauthors, 2012: Observation and modelling of OH and HO_2 concentrations in the Pearl River Delta 2006: A missing OH source in a VOC rich atmosphere. *Atmos. Chem. Phys.*, **12**, 1541–1569.

Ma, J. Z., and Coauthors, 2012: The IPAC-NC field campaign: A pollution and oxidization pool in the lower atmosphere over Huabei, China. *Atmos. Chem. Phys.*, **12**, 3883–3908.

Mao, J., and Coauthors, 2009: Airborne measurement of OH reactivity during INTEX-B. *Atmos. Chem. Phys.*, **9**, 163–173.

Ohara, T., H. Akimoto, J. Kurokawa, N. Horii, K. Yamaji, X. Yan, and , T. Hayasaka, 2007: An Asian emission inventory of anthropogenic emission sources for the period 1980–2020. *Atmos. Chem. Phys.*, **7**, 4419–4444.

Palmer, P. I., D. J. Jacob, A. M. Fiore, R. V. Martin, K. Chance, and T. P. Kurosu, 2003: Mapping isoprene emissions over North America using formaldehyde column observations from space. *J. Geophys. Res.*, **108**, 4180, doi: 10.1029/2002JD002153.

Palmer, P. I., and Coauthors, 2006: Quantifying the seasonal and interannual variability of North American isoprene emissions using satellite observations of the formaldehyde column. *J. Geophys. Res.*, **111**, D12315, doi: 10.1029/2005JD006689.

Shao, M., X. Tang, Y. Zhang, and W. Li, 2006: City clusters in China: Air and surface water pollution. *Frontiers in Ecology and the Environment*, **4**, 353–361.

Shao, M., S. Lu, Y. Liu, X. Xie, C. Chang, S. Huang, and Z. Chen, 2009: Volatile organic compounds measured in summer in Beijing and their role in ground-level ozone formation. *J. Geophys. Res.*, **114**, D00G06, doi:10.1029/2008JD010863.

Shirley, T., and Coauthors, 2006: Atmospheric oxidation in the Mexico City metropolitan area (MCMA) during April 2003. *Atmos. Chem. Phys.*, **6**, 2753–2765.

Sillman, S., 1999: The relation between ozone, NO_x and hydrocarbons in urban and polluted rural environments. *Atmos. Environ.*, **33**, 1821–1846.

Sillman, S., and D. Y. He, 2002: Some theoretical results concerning O_3-NO_x-VOC chemistry and NO_x-VOC indicators. *J. Geophys. Res.*, **107**, 4659, doi: 10.1029/2001JD001123.

Simon, H., K. R. Baker, and S. Phillips, 2012: Compilation and interpretation of photochemical model performance statistics published between 2006 and 2012. *Atmos. Environ.*, **61**, 124–139.

Song, S.-K., Y.-K. Kim, Z.-H. Shon, and J.-Y. Ryu, 2012: Photochemical analyses of ozone and related compounds under various environmental conditions. *Atmos. Environ.*, **47**, 446–458.

Streets, D., and Coauthors, 2003: An inventory of gaseous and primary aerosol emissions in Asia in the year 2000. *J. Geophys. Res.*, **108**, 8809, doi: 10.1029/2002JD003093.

Tang, Y., J. An, Y. Li, and F. Wang, 2014: Uncertainty in the uptake coefficient for HONO formation on soot and its impacts on concentrations of major chemical components in the Beijing–Tianjin–Hebei region. *Atmos. Environ.*, **84**, 163–171.

Thornton, J., and Coauthors, 2002: Ozone production rates as a function of NO_x abundances and HO_x production rates in the Nashville urban plume. *J. Geophys. Res.*, **107**, 4146, doi: 10.1029/2001jd000932.

Tie, X., F. Geng, L. Peng, W. Gao, and C. Zhao, 2009: Measurement and modeling of O_3 variability in Shanghai, China: Application of the WRF-Chem model. *Atmos. Environ.*, **43**, 4289–4302.

Tonooka, Y., and Coauthors, 2001: NMVOCs and CO emission inventory in East Asia. *Water Air and Soil Pollution*, **130**, 199–204.

Wang, X., and Coauthors, 2010: Process analysis and sensitivity study of regional ozone formation over the Pearl River Delta, China, during the PRIDE-PRD2004 campaign using the Community Multiscale Air Quality modeling system. *Atmos. Chem. Phys.*, **10**, 4423–4437.

Wei, W., S. Wang, S. Chatani, Z. Klimont, J. Cofala, and J. Hao, 2008: Emission and speciation of non-methane volatile organic compounds from anthropogenic sources in China. *Atmos. Environ.*, **42**, 4976–4988.

Xing, J., S. X. Wang, C. Jang, Y. Zhu, and J. M. Hao, 2011: Nonlinear response of ozone to precursor emission changes in China: A modeling study using response surface methodology. *Atmos. Chem. Phys.*, **11**, 5027–5044.

Xu, X. B., B. Z. Ge, and W. L. Lin, 2009: Progresses in the Research of Ozone Production Efficiency (OPE). *Advances in Earth Science*, **24**, 845–853.

Zare, A., J. Brandt, J. H. Christensen, and P. Irannejad, 2012: Evaluation of two isoprene emission models for use in a long-range air pollution model. *Atmos. Chem. Phys. Discuss.*, **12**, 9247–9281.

Zaveri, R. A., and L. K. Peters, 1999: A new lumped structure photochemical mechanism for large-scale applications. *J. Geophys. Res.*, **104**, 30387–30415.

Zaveri, R. A., R. C. Easter, J. D. Fast, and L. K. Peters, 2008: Model for simulating aerosol interactions and chemistry (MOSAIC). *J. Geophys. Res.*, **113**, D13204, doi:10.1029/2007JD008782.

Zhang, H., and Coauthors, 2012: Source apportionment of $PM_{2.5}$ nitrate and sulfate in China using a source-oriented chemical transport model. *Atmos. Environ.*, **62**, 228–242.

Zhang, Q., and Coauthors, 2009: Asian emissions in 2006 for the NASA INTEX-B mission. *Atmos. Chem. Phys.*, **9**, 5131–5153.

Zhang, Y., and Coauthors, 2008: Regional integrated experiments on air quality over Pearl River Delta 2004 (PRIDE-PRD2004): Overview. *Atmos. Environ.*, **42**, 6157–6173.

Zhao, Y., S. Wang, C. P. Nielsen, X. Li, and J. Hao, 2010: Establishment of a database of emission factors for atmospheric pollutants from Chinese coal-fired power plants. *Atmos. Environ.*, **44**, 1515–1523.

Zheng, J., L. Zhang, W. Che, Z. Zheng, and S. Yin, 2009: A highly resolved temporal and spatial air pollutant emission inventory for the Pearl River Delta region, China and its uncertainty assessment. *Atmos. Environ.*, **43**, 5112–5122.